

# The distribution of glass-transition temperatures in nanoscopically confined glass formers

CHRISTOPHER J. ELLISON<sup>1</sup> AND JOHN M. TORKELSON<sup>\*1,2</sup>

<sup>1</sup>Department of Chemical Engineering and <sup>2</sup>Department of Materials Science and Engineering, Northwestern University, Evanston, Illinois 60208-3120, USA

\*e-mail: j-torkelson@northwestern.edu

Published online: 21 September 2003; doi:10.1038/nmat980

Despite the decade-long study of the effect of nanoconfinement on the glass-transition temperature ( $T_g$ ) of amorphous materials, the quest to probe the distribution of  $T_g$ s in nanoconfined glass formers has remained unfulfilled. Here the distribution of  $T_g$ s across polystyrene films has been obtained by a fluorescence/multilayer method, revealing that the enhancement of dynamics at a surface affects  $T_g$  several tens of nanometres into the film. The extent to which dynamics smoothly transition from enhanced to bulk states depends strongly on nanoconfinement. When polymer films are sufficiently thin that a reduction in thickness leads to a reduction in overall  $T_g$ , the surface-layer  $T_g$  actually increases with a reduction in overall thickness, whereas the substrate-layer  $T_g$  decreases. These results indicate that the gradient in  $T_g$  dynamics is not abrupt, and that the size of a cooperatively rearranging region is much smaller than the distance over which interfacial effects propagate.

The nature of the glass transition is considered a major intellectual challenge in condensed-matter physics<sup>1–3</sup>. Since the discovery a decade ago of the deviation from bulk values of the glass-transition temperature ( $T_g$ ) due to nanoconfinement<sup>4–6</sup>, there has been intense interest in characterizing and understanding the impact of nanoconfinement in modifying the  $T_g$  of low-molecular-weight and polymeric glass formers. This interest has included attempts to make a quantitative connection between the length scale of an average cooperatively rearranging region (CRR), and the length scale at which nanoconfinement effects are observed<sup>7</sup>. In the picture of Adam and Gibbs<sup>8</sup>, local relaxation occurs in a CRR by collective motion of many small molecules or polymer segments. The accepted size of a CRR near  $T_g$  ranges<sup>9,10</sup> from 1 to 4 nm. However, the length scale at which confined glass formers deviate from bulk  $T_g$  is typically larger than the size of a CRR. For low-molecular-weight glass formers, this length scale ranges from several nanometres to several tens of nanometres<sup>4,11–14</sup>. For polymers, it ranges from tens of nanometres (<100 nm) in the absence of attractive substrate interactions<sup>6,7,14–19</sup> to values exceeding 100 nm in the presence of strongly attractive substrate interactions<sup>16</sup>.

Despite the many scientific studies<sup>7,15</sup> devoted to the modification of glass-transition dynamics by nanoconfinement, and the many models<sup>7,15–17,19–25</sup> that have been constructed to fit or explain experimental data, a fundamental understanding of the origin of this nanoconfinement effect has not yet been realized. In a recent note on the impact of thickness on  $T_g$  values in thin polymer films, de Gennes<sup>21</sup> stated “future experiments should aim not at the determination of a single  $T_g$ , but at a distribution of  $T_g$ s.” An accompanying commentary by Jones<sup>26</sup> stated, “The picture of a local glass transition that effectively depends on the depth from the surface needs to be tested directly, rather than inferred from the global behaviour of thin films. This is a formidably difficult requirement, but the potential rewards, both in terms of an improved understanding of the nature of the glass transition, and in a better understanding of practically important properties of glassy polymers . . . are substantial.” Here we report the first determination of the distribution of  $T_g$ s within thin and ultrathin polymer films through fluorescence, allowing characterization of  $T_g$  within surface, interior and substrate layers of known thickness.

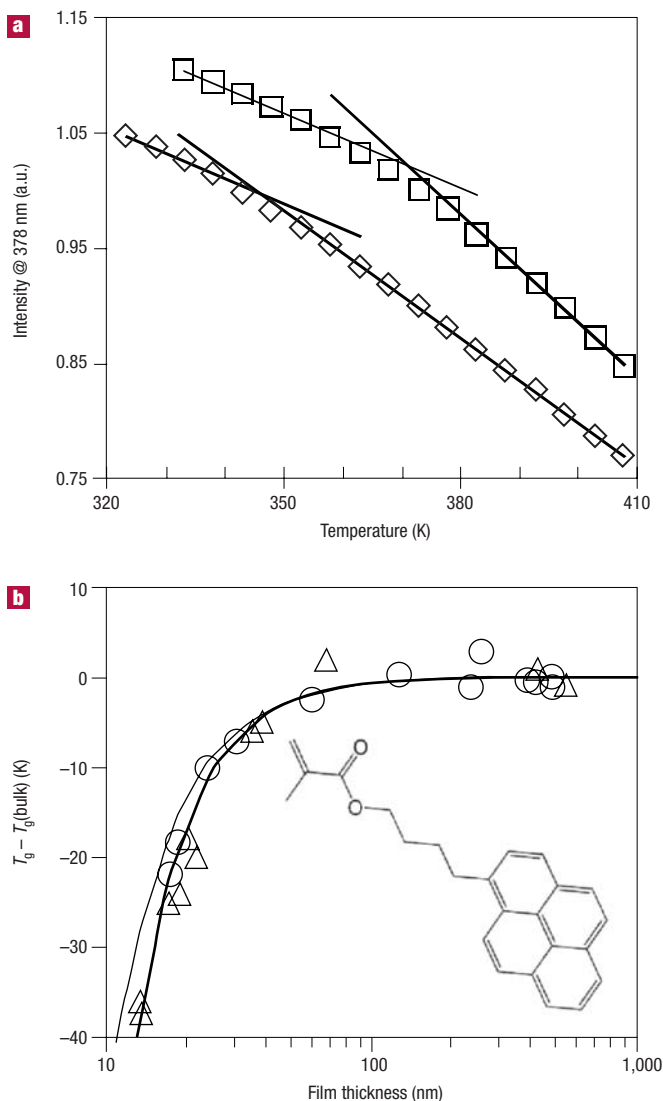


**Figure 1**  $T_g$  of single-layer PS films identified by fluorescence using pyrene as dopant or label. **a**, Temperature dependence of fluorescence for pyrene-labelled PS single-layer films: 545-nm thick (squares) and 17-nm thick (diamonds). Intensities are normalized to 373 K and arbitrarily shifted vertically for clarity. a.u. = arbitrary units. **b**, Thickness dependence of  $T_g$  to pyrene-doped (circles) and pyrene-labelled (triangles) PS films. The bold curve is a least-squares fit of equation (1) for pyrene-doped data ( $A = 4.3$ ,  $\delta = 2.0$ ,  $T_g(\text{bulk}) = 373$  K) reported previously in ref. 31; the thin curve is a reproduction of the fit reported by Keddie *et al.*<sup>6</sup> in their ellipsometry study of PS  $T_g$ -nanoconfinement effects ( $A = 3.2$ ,  $\delta = 1.8$ ,  $T_g(\text{bulk}) = 374$  K).  $T_g(\text{bulk}) = 371$  K for pyrene-labelled PS. The inset shows the structure of 1-pyrenyl butyl methacrylate used for labelling PS.

The decision to pursue the characterization of the distribution of  $T_g$ s in nanoconfined polymer films as opposed to low-molecular-weight glass formers is due to several factors. First, polymer films dominate  $T_g$ -nanoconfinement studies because the confining dimension (film thickness) is easily tuned by spin-coating<sup>27</sup>. Thickness-dependent  $T_g$ s have been measured by ellipsometry<sup>6,15</sup>, X-ray reflectivity<sup>16</sup>, dielectric spectroscopy<sup>17</sup>, Brillouin scattering<sup>18</sup> and other methods<sup>19,28–32</sup>. The most commonly studied system is polystyrene (PS) supported on silicon or silica substrates, and recent reviews<sup>7,15</sup> have found considerable agreement among the many studies of this system, supporting the empirical relation<sup>6</sup>:

$$T_g(h) = T_g(\text{bulk})[1 - (A/h)^\delta] \quad (1)$$

where  $h$  is film thickness,  $A$  is a characteristic length (3.2 nm),  $\delta = 1.8$ , and  $T_g(\text{bulk}) = 374$  K.

Second, various models<sup>7,15–17,19–25</sup> have addressed the  $T_g$  depression of nanoconfined polymer films, with many being two- or three-layer models. In simple two-layer models, the free-surface layer has enhanced mobility and reduced  $T_g$  relative to the rest of the film that is assumed to exhibit bulk  $T_g$ <sup>7,15,17,23</sup>. In three-layer models, a substrate-interface layer is added to the two-layer model. This third layer may be considered to be “dead”<sup>19</sup>, exhibiting no  $T_g$  over the temperature range of interest, or may have an elevated  $T_g$  relative to bulk  $T_g$ <sup>23</sup>, the latter of which may apply to films that exhibit attractive interactions with the substrate. Such models can be used to fit data, with two- and three-layer models describing systems with  $T_g$ s that decrease monotonically with decreasing overall thickness; three-layer models that incorporate an elevated  $T_g$  near the substrate can even describe systems that exhibit an initial reduction in  $T_g$  with decreasing overall thickness followed, at some critical thickness, by an increase in  $T_g$  with a yet further decrease in thickness<sup>23</sup>. However, although such models can fit data, they do not afford a fully critical examination of the impact of nanoconfinement on  $T_g$ . The combination of substantial experimental agreement for the  $T_g$  depression in nanoconfined, supported PS films, and the existence of basic multilayer models attempting to explain these results, allow for straightforward comparison with results obtained on the distribution of  $T_g$ s through fluorescence measurements using multilayer PS films. Finally, it is important to note that parallel experiments that probe the distribution of  $T_g$ s in well-defined regions in confined low-molecular-weight glass formers would not be possible. (An implanted ion mobility method has been reported<sup>33</sup> that probes the distribution of viscosities in well-defined regions of confined low-molecular-weight glass formers. However, this method probes viscosity within a few orders of magnitude of  $10^5$  poise, characteristic of temperatures substantially above  $T_g$ .) Despite this fact, the results presented here are expected to have general applicability to all confined glass formers.

Ensemble and single-molecule fluorescence have been used to study  $T_g$ -related issues in single-layer polymer films<sup>31,32,34,35</sup>. With ensemble fluorescence<sup>31,32</sup>,  $T_g$  is identified by a shift in the temperature ( $T$ ) dependence (measured on cooling) of the fluorescence of pyrene that is doped into or covalently attached (labelled) to the polymer at trace levels. Pyrene is well suited as a chromophore in nanoconfined PS due to its high extinction coefficient and fluorescence quantum yield. Figure 1a shows the  $T$ -dependence of the fluorescence of pyrene-labelled PS where pyrene is incorporated into PS by polymerizing styrene with low levels of 1-pyrenyl butyl methacrylate, yielding PS with 0.59 mol% pyrenyl butyl methacrylate ( $M_n = 440$  kg mol<sup>-1</sup>;  $M_w/M_n = 1.73$ ). The  $T_g$  identified by the intersection of linear fits to the liquid- and glassy-state  $T$ -dependences, decreases from 370 K to 346 K as thickness is reduced from 545 nm to 17 nm. There is also a reduced difference between the liquid- and glassy-state slopes in the ultrathin film indicating a reduction in the strength of the glass transition upon nanoconfinement, behaviour also seen in ref. 15.

Figure 1b shows that the thickness dependences of  $T_g - T_g(\text{bulk})$  obtained by fluorescence of pyrene-labelled and pyrene-doped (< 0.2 wt% dopant) PS films are essentially identical and agree with previous results<sup>6</sup>. For pyrene-labelled PS,  $T_g(\text{bulk})$  by fluorescence is 371 K, in agreement with  $T_g$  by differential scanning calorimetry (DSC) ( $T(\text{onset}) = 369$  K,  $T_g(1/2\Delta C_p) = 372$  K, where  $C_p$  is the specific heat capacity). This indicates that fluorescence of pyrene-doped or -labelled PS provides meaningful characterization of  $T_g$  and that there is no substantial partitioning of pyrene to the substrate or free surface.

Why is pyrene fluorescence sensitive to polymer  $T_g$ ? Pyrene fluorescence does not provide sensitivity to the  $\alpha$ -relaxation (cooperative segmental mobility, the relaxation associated with  $T_g$ ) due

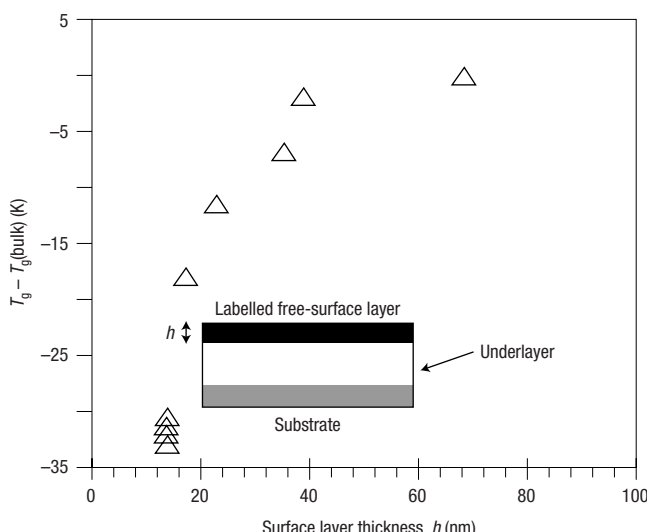


**Figure 2**  $T_g - T_g(\text{bulk})$  identified by fluorescence for pyrene-labelled PS free-surface layers of variable thickness placed on top of constant bulk-like (~270 nm) unlabelled PS underlayers.

to the large mismatch between the chromophore excited-state lifetime (~200 ns, ref. 36) and the average  $\alpha$ -relaxation time at  $T_g$  (~100 s, ref. 37). Instead, the  $T$ -dependence of the fluorescence of pyrene-doped or -labelled PS may be understood as follows: Fluorescence from the excited state of pyrene is in competition with non-radiative decay occurring by vibrational and other modes. The rate of non-radiative decay increases with increasing temperature, leading to a decrease in fluorescence. Superimposed on this is sensitivity to local density of the nanoscale environment surrounding the chromophore, with a slightly denser environment accommodating less non-radiative decay, leading to higher intensity. The shift in the  $T$ -dependence of intensity at  $T_g$  is thus a result of the shift in the  $T$ -dependence of sample density.

Fluorescence of labelled PS confined within a film of known thickness has been exploited to measure  $T_g$  at specific locations within multilayer PS films. These films contain a single, labelled layer and one or two unlabelled PS layers ( $M_n \sim 400 \text{ kg mol}^{-1}$ ). By heating the layered films for short time periods above  $T_g$ , the layers fuse, producing a continuous film with label only at particular depths within the film. The effectiveness of the multilayer fusion is proven by comparison of the  $T_g$  values of a single 14-nm-thick labelled PS film on a glass substrate and a 14-nm-thick labelled PS film sandwiched between two 270-nm-thick unlabelled PS films. The single 14-nm-thick film has a  $T_g$  that is 37 K below bulk  $T_g$ , whereas the 14-nm-thick layer in the fused, three-layer sandwich exhibits bulk  $T_g$ .

The labelled and unlabelled PS chains are of sufficiently high molecular weight to ensure that the labelled PS diffuses, at most, several nanometres during measurement. The expected interpenetration distance of these layers may be estimated based on secondary ion mass spectroscopy (SIMS) data<sup>38</sup>. For the materials and conditions used in this study (that is, annealing at 403 K for 10 min before taking fluorescence measurements), the average repeat-unit interpenetration depth ( $X(t)$  where  $t$  is the annealing or diffusion time) is much less than the radius of gyration ( $R_g$ ) ( $R_g \sim 17 \text{ nm}$  for PS of  $M_n = 400 \text{ kg mol}^{-1}$  used in this study), and therefore the diffusion time is less than the reptation time<sup>38</sup>. Under these conditions  $X(t)$  follows the scaling relationship<sup>38</sup>  $X(t) \sim t^{(1/4)} M^{(-1/4)}$ . Using SIMS interlayer diffusion data for 591  $\text{kg mol}^{-1}$  PS and 693  $\text{kg mol}^{-1}$  deuterated PS annealed at 418 K and 90 min

( $X(t) = 14.0 \text{ nm}$  for this case)<sup>38</sup>, it can be estimated that for this fluorescence study using PS layers with  $M_n \sim 400 \text{ kg mol}^{-1}$  at 418 K for 10 min would yield an expected  $X(t)$  of 6 nm. This is an upper bound for the expected interlayer penetration of this study, as the annealing temperatures used in this fluorescence study are 15 K less than those used for estimation. In addition, both in-plane<sup>39</sup> and out-of-plane<sup>40</sup> polymer diffusion have been reported to be reduced relative to that of bulk systems even in films as thick as 100 nm (ref. 40), reiterating that these estimated values are upper limits. Thus, fluorescence can provide the first determination of the distribution of  $T_g$ s at well-defined locations across thin polymer films.

Using this novel approach, data were obtained showing how  $T_g$  varies as a function of thickness of the free-surface layer of a supported, bulk PS film. PS films of known thickness were floated onto the surface of 270-nm-thick unlabelled PS films supported on glass. The overall film was sufficiently thick to exhibit bulk  $T_g$ . Figure 2 shows that a 14-nm-thick free-surface layer yields  $T_g - T_g(\text{bulk}) = \sim -32 \text{ K}$ . Examining yet thicker surface layers shows that  $T_g$  varies smoothly with surface-layer thickness, with this layer exhibiting bulk  $T_g$  when its thickness exceeds a value in the range of 40–70 nm. PS surface-layer  $T_g$ s have reportedly been measured with thicknesses similar to those in Fig. 2; using Doppler broadening energy spectra of positron annihilation, Jean *et al.*<sup>41</sup> found that  $T_g - T_g(\text{bulk}) = -19 \text{ K}$  for a surface layer that can be interpreted to have a 22-nm “mean penetration depth”. The substantially reduced  $T_g$  in the surface layer is also qualitatively consistent with recent studies<sup>30,42,43</sup>, indicating that the segmental mobility near the surface of a PS film is significantly faster than in bulk PS, but in disagreement with the conclusion reached in an earlier study<sup>44</sup> that the polymer segmental mobility at a free surface and in the bulk are not significantly different.

According to Fig. 2, the  $T_g$  of a 14-nm-thick labelled surface layer on a bulk film is ~5 K higher than the  $T_g$  of a 14-nm-thick single-layer film (see Fig. 1b). This indicates that having layers with bulk dynamics underneath the surface layer can slow the dynamics and lead to a higher

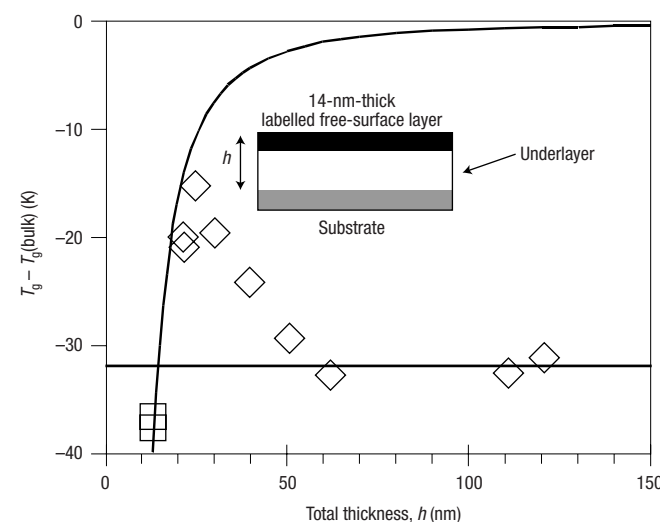


**Figure 3**  $T_g$  identified by fluorescence for 14-nm-thick pyrene-labelled PS free-surface layers (diamonds) as a function of total film thickness where the underlayer thickness is varied. The solid curve is the fit of equation (1) to the thickness dependence of single-layer pyrene-doped PS data in Fig. 1b. In addition, two replicate single-layer  $T_g$ s for 14-nm-thick labelled PS films (squares) are shown for reference. The horizontal line represents the value at which  $T_g - T_g(\text{bulk})$  of the 14-nm-thick free-surface layer is independent of underlayer thickness.

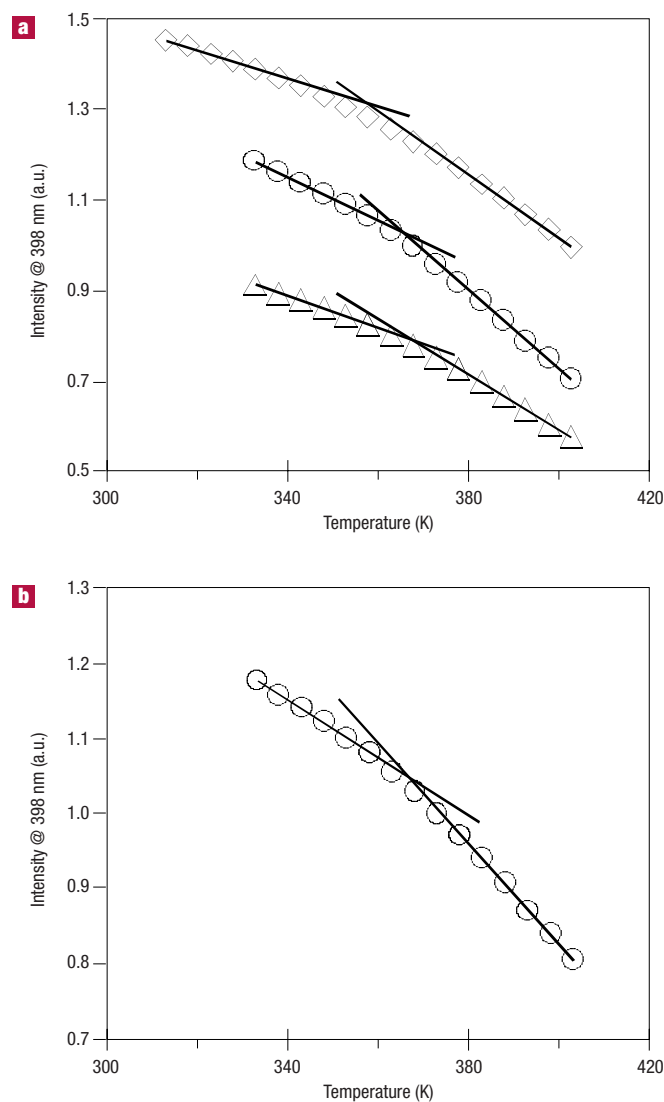


**Figure 4**  $T_g$  identified by fluorescence for a three-layer PS film (each layer 12-nm thick, only one pyrene-labelled layer). **a**, Temperature dependence of fluorescence intensity of the substrate layer (triangles), middle layer (circles) and free-surface layer (diamonds). All data have been normalized to 373 K and arbitrarily shifted vertically for clarity. **b**, Normalized sum of the temperature dependences of fluorescence intensity for all three (substrate, middle and free-surface) 12-nm-thick layers.

surface-layer  $T_g$  relative to that of a single-layer film of thickness identical to the surface layer. It is also noteworthy that a broadened  $T_g$  (that is, an increasing range of temperature over which the  $T$ -dependence of fluorescence intensity deviates from the linear rubbery- and glassy-state  $T$ -dependences) is observed with decreasing thickness of the free-surface layer. In bulk films, free-surface layers of 69 nm, 35 nm and 14 nm thickness exhibit  $T_g$  breadths of 15–20 K, 20–25 K and 40–45 K, respectively. The increasing breadth in  $T_g$  with decreasing free-surface layer thickness indicates that the strongest gradient in  $T_g$  is nearest the free surface.

Studies were also done on two-layer films with ultrathin, labelled PS films as the substrate layer and a 270-nm-thick unlabelled PS cover layer. Within error, the substrate layer  $T_g$  is equal to bulk  $T_g$  down to

substrate-layer thicknesses of 12 nm. The details of how the thickness of the underlayer to a 14-nm-thick free-surface layer affects the  $T_g$  of the surface layer are shown in Fig. 3. When the total film thickness exceeds 60 nm, the surface layer exhibits a  $T_g$  that is 32 K below bulk  $T_g$ . However, as total film thickness decreases below 60 nm and approaches 25 nm, there is a sharp rise in the surface layer  $T_g$ . For total film thickness below 25 nm, the 14-nm-thick surface layer exhibits a  $T_g$  value that is within error identical to that of the average  $T_g$  across the whole film. These results show that between certain total thicknesses (25–60 nm) the mobile surface layer becomes less mobile with decreasing film thickness and decreasing average  $T_g$  across the whole film. At a total thickness below 25 nm, it is impossible to distinguish through  $T_g$  values a mobile 14-nm-thick surface layer from the remainder of the film.

The results above disallow the premises associated with simple two- and three-layer models that do not account for a smooth gradient in cooperative dynamics across a film thickness, or for the dependence of surface- and substrate-layer cooperative dynamics on the extent of nanoconfinement. Instead, to understand the impact of nanoconfinement on  $T_g$ , Fig. 3 indicates that one must appreciate that the average cooperative dynamics associated with  $T_g$  at a particular film depth are impacted by the average cooperativity present in layers several tens of nanometres away from the layer of interest. That is, the most important length scale is not the size defining an average CRR but rather is the distance over which a perturbation in cooperative dynamics at one location, for example, the free-surface layer, affects the dynamics elsewhere in the film. Thus, if on average the cooperative dynamics in a layer are perturbed to be substantially enhanced relative to bulk (as at a free surface), then, on average, adjoining layers must also have their dynamics perturbed, albeit to a lesser extent.

This picture is consistent with simulations<sup>45</sup> and experiments<sup>46</sup> on colloidal glass formers indicating that regions of very fast dynamics are clustered such that a fast moving particle is unlikely to be adjacent to particles with very slow dynamics. That is, glass formers do not normally have abrupt, local spatial transitions from very fast dynamics to very slow dynamics. Indirect experimental support for this picture is also provided by X-ray reflectivity studies<sup>47</sup> of ultrathin (<10 nm thick) liquid films of nearly spherical, non-polar molecules that reveal a gradient in local density, which should be related to local dynamics<sup>24</sup>, over a number molecular layers near an interface. This picture is also consistent with single-molecule fluorescence and dielectric-noise studies<sup>35,48</sup> that yield estimates of the minimum length scale (>40 nm, ref. 48, possibly ~100 nm, ref. 35) that contains the full breadth of the distribution of cooperative relaxation dynamics in polymers near  $T_g$ . If this length scale is at least several tens of nanometres, it may be speculated that a substantial perturbation to average cooperative dynamics at a film surface could perturb average cooperative dynamics at a film depth of similar length, leading to  $T_g$ -nanoconfinement effects. Further study is warranted of the possible connection between the length scale encompassing the full breadth of the distribution of cooperative relaxation dynamics in bulk glass formers and the length scale at which  $T_g$ -nanoconfinement effects become evident.

Determination of the length scale over which a perturbation of average cooperative dynamics at a surface can modify dynamics within a film was made using three-layer films (total thickness >290 nm), with a 14-nm-thick, pyrene-labelled PS middle layer. With a 7- to 9-nm-thick cover layer of unlabelled PS, the middle-layer  $T_g$  is depressed by 7 K relative to bulk. With a 12- to 15-nm-thick cover layer of unlabelled PS, the middle-layer  $T_g$  is depressed by 3 K relative to bulk, meaning that a reduction in  $T_g$  relative to bulk can be quantified at layer depths up to ~30 nm from the film surface. When the cover layer exceeds a thickness in the range of 18–30 nm (maximum middle-layer depth range of 32–44 nm), within error the middle layer exhibits bulk  $T_g$ . Thus, as with the surface layer study in Fig. 2, a 14-nm-thick middle layer in a bulk three-layer film shows a smooth variation in  $T_g$ .

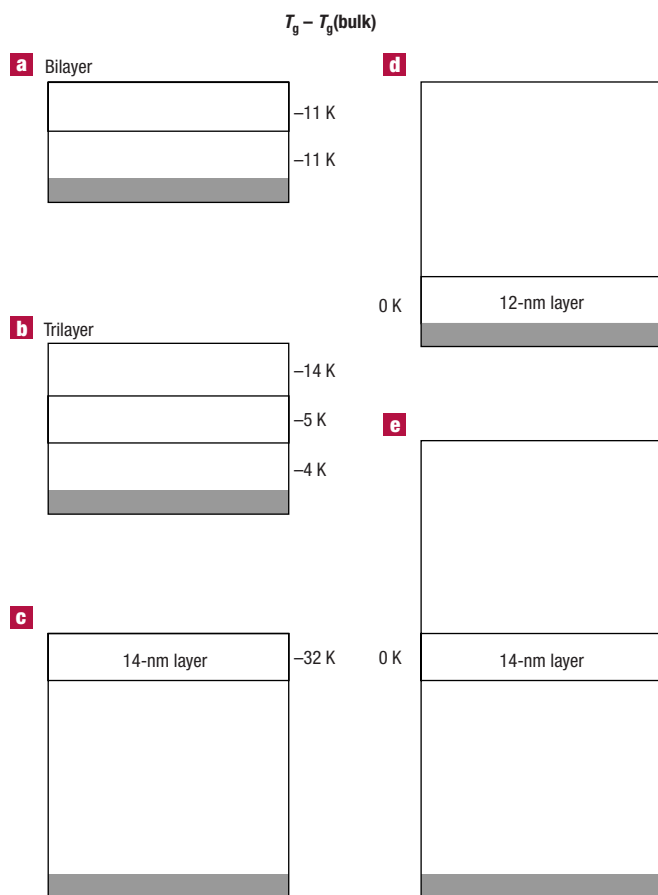


**Figure 5** Summary of  $T_g - T_g(\text{bulk})$  for single pyrene-labelled PS layers inserted at specific locations in unlabelled PS films.  $T_g - T_g$  for single 12-nm-thick labelled layers in **a**, bilayer films (24 nm in total thickness) with the labelled layer at either the substrate or the free surface, or **b**, trilayer films (36 nm in total thickness) with the labelled layer at the substrate, middle or free surface.  $T_g - T_g(\text{bulk})$  for **c**, a 14-nm-thick labelled free-surface layer with a ~270 nm neat PS underlayer, **d**, a 12-nm-thick labelled substrate layer with a ~270 nm neat PS overlayer and **e**, a 14-nm-thick labelled middle layer with ~270 nm neat PS layers on each side.

as it is located deeper into the film, exhibiting bulk  $T_g$  only at a depth exceeding a few tens of nanometres.

Two other questions can be addressed with multilayer films. First, is it logical that the apparent  $T_g$  of an ultrathin PS film can yield a single, definable  $T_g$  when the surface layer exhibits a  $T_g$  substantially different from portions of the film closer to the substrate? Second, when the films are below a critical thickness, such that the length scale required to achieve a smooth transition from a highly mobile, free-surface layer to a bulk-like layer near the substrate exceeds that of the total film, how will the surface and substrate layers be impacted? These questions are answered by multilayer film studies (12-nm-thick layers, one labelled layer per film). Figure 4 shows the  $T$ -dependences of fluorescence obtained from the free-surface, middle and substrate-interface layers in a three-layer film as well as the sum of the intensities from all three layers, the latter yielding the total film  $T_g$ . The surface, middle and substrate layers have  $T_g$  depressions relative to bulk of 14 K, 5 K and 3 K, respectively. (Note that the free-surface layer in Fig. 4a has a broadened  $T_g$  with a breadth of approximately 40–45 K, in reasonable agreement

with the breadth of the 14-nm-thick free-surface layers of Fig. 2.) When the three layer intensities are summed,  $T_g - T_g(\text{bulk}) = -5$  K, within 1 K of that obtained for a 36-nm-thick, single-layer film (see Fig. 1b). Thus, in films as thin as 36 nm where there is a substantial reduction in the  $T_g$  of the overall film from bulk, the surface layer (one third of the total thickness) can have a  $T_g$  depressed by 9 K or more relative to the rest of the film, whereas the overall  $T_g$  is close to those of the non-surface layers. In contrast, with a two-layer, 24-nm-thick film, the overall film is so thin that both 12-nm-thick layers are constrained to have identical  $T_g - T_g(\text{bulk})$  values (−11 K) in reasonable agreement with that of a single 24-nm-thick film (see Fig. 1b).

Relative to thicker films exhibiting bulk  $T_g$ , there is a significant narrowing of the range of  $T_g$ s obtained in the layers of the 36-nm-thick, three-layer film; the surface layer exhibits a  $T_g$  that is ~18 K higher than when a surface layer of similar thickness is on a bulk film, and the substrate layer exhibits a  $T_g$  that is 3 K lower than when a similar layer is part of a bulk film. (A summary of these results is given in Fig. 5.) Thus, a total thickness exceeding 36 nm is required for a smooth transition from highly enhanced, average cooperative dynamics on a surface layer of a bulk PS film to bulk dynamics. If the total thickness is below a critical value (Fig. 3 suggests ~60 nm), the dynamics adjust to satisfy the constraint that the gradient in average cooperative dynamics from surface to substrate is not too sharp and abrupt. When the total thickness is below a second critical value, seen from Fig. 3 to be 25 nm when using a 14-nm-thick labelled layer, within error there is one  $T_g$  regardless of layer location. Below 25 nm, there is an insufficient length scale to accommodate a substantial, smooth gradient in average cooperative dynamics from surface to substrate.

In summary, this is the first report of the determination of the distribution of  $T_g$ s in nanoconfined polymers. With a supported PS film, the distance over which a diminishing level of enhanced mobility extends into the film from the surface is several tens of nanometres, and the extent to which the surface-layer mobility is enhanced relative to the rest of the film depends strongly on the level of nanoconfinement of the whole film. This indicates that the most important length scale defining the  $T_g$ -nanoconfinement effect is the distance over which a perturbation in average cooperative dynamics at one location, for example, the surface, affects the cooperative dynamics elsewhere in the polymer. Studies to establish a relationship between this length scale and the length scale of an average CRR are underway.

## METHODS

### MATERIALS SYNTHESIS AND CHARACTERIZATION

Pyrene-labelled methacrylate monomer was synthesized by esterification of methacryloyl chloride (Aldrich) and 1-pyrenyl butanol (Aldrich). Polymerization of labelled and unlabelled polystyrene (PS) was initiated with benzoyl peroxide (Aldrich) in test tubes immersed in a water bath at 75 °C in an air atmosphere. All polymers were thoroughly washed by dissolving in toluene and precipitating in methanol at least five times to remove any residual monomer, and placed in a vacuum oven at 105 °C for 3 days before use. Labelled PS was synthesized by addition of 0.67 mol% labelled methacrylate monomer to styrene producing a polymer where approximately 1 in 170 units (0.59 mol%) are a labelled methacrylate (by UV-VIS absorbance, Perkin Elmer Lambda 35) and effective labelling was verified through fluorescence-detection gel permeation chromatography (GPC, Waters Breeze). Molecular weight distributions were characterized by GPC using PS standards and refractive index, absorbance and fluorescence detection. The calorimetric  $T_g$  was determined by DSC (Mettler Toledo DSC 822e) reported as the onset temperature or  $1/2\Delta C_p$  on second heat at a heating rate of 10 K min<sup>-1</sup>. The labelled PS used in this study had  $M_n = 440$  kg mol<sup>-1</sup> and  $M_w = 760$  kg mol<sup>-1</sup> (bulk DSC  $T_g(\text{onset}) = 369$  K,  $T_g(1/2\Delta C_p) = 372$  K), and the unlabelled PS used in multilayer film studies was either synthesized having  $M_n = 419$  kg mol<sup>-1</sup> and PDI = 1.73, where PDI =  $M_w/M_n$  (bulk DSC  $T_g(\text{onset}) = 369$  K,  $T_g(1/2\Delta C_p) = 372$  K) or purchased (Pressure Chemical) having a nominal  $M_n = 400$  kg mol<sup>-1</sup> and PDI = 1.06 (bulk DSC  $T_g(\text{onset}) = 374$  K,  $T_g(1/2\Delta C_p) = 378$  K). PS used in pyrene-doped film studies was used as received from Pressure Chemical ( $M_n = 263$  kg mol<sup>-1</sup>, PDI = 1.10 measured by GPC, bulk DSC  $T_g(\text{onset}) = 373$  K).

### PRODUCTION OF SINGLE-LAYER AND MULTILAYER FILMS

PS films were spin-coated onto NaCl infrared crystal windows (Aldrich) or glass substrates from solutions of toluene where the thickness was varied by changing solution concentration and spin speed. Films were transferred to a glass substrate or placed on top of another polymer film (when forming multilayer films) by floating them from the salt disk in a large water reservoir. Film thickness was verified by spin-coating a second film at the same time from the same solution (in addition to the film spin-coated on the salt disk) onto a glass substrate and measuring its thickness by profilometry (Tencor P10).

Calibration of the profilometer was verified using a 14-nm step-height standard (VLSI Standards). Vertical instrument resolution was set to 2 Å as reported by the manufacturer. At least ten measurements of the film thickness were made (more than ten measurements were made for films  $< 15$  nm) near the centre of the film and averaged (average value is reported in the main text) with the typical standard deviation in these measurements being less than 1.5 nm for films thicker than  $\sim 20$  nm and less than 1.0 nm for films thinner than  $\sim 20$  nm. Multilayer films were made by spin-coating individual layers onto different salt disks and sequentially floating them onto the substrate or underlying polymer layers. In between the placement of each layer, excess water was allowed to evaporate under ambient conditions before the next layer was added. On completion, all films were placed in a vacuum oven at room temperature for at least 12 h prior to measurement.

#### MEASUREMENT OF $T_g$ USING A FLUORESCENCE TECHNIQUE

The  $T_g$  was identified by the intersection of linear fits to the rubbery- and glassy-state temperature dependences of the fluorescence emission intensity. Fluorescence was measured with a SPEX Fluorolog-2 DM1B fluorimeter. The chromophore pyrene, either as label (all Figs) or dopant (part of Fig. 1b), was used as the fluorescence sensor of  $T_g$  in all cases discussed. Pyrene was labelled or doped (dopant content  $< 0.2$  wt%) at sufficiently low content such that the  $T_g$  of identical neat or unlabelled PS was within  $\sim 1$  K of that containing pyrene. Fluorescence measurements were taken on a Spex Fluorolog-2 DM1B fluorimeter in the front-face geometry with 2.5-mm excitation and emission slits (bandpass = 4.5 nm). For the case of pyrene doped into PS, the excitation wavelength was set to 322 nm, and the emission intensity was monitored at 374, 384 and 395 nm; for pyrene-labelled PS, the excitation wavelength was set to 340 nm, and the emission intensity was monitored at 378 nm and 398 nm. All  $T_g$  measurements represent an average of the intersection of the linear fits (only data points well outside  $T_g$  were used for the linear fits and typical correlations ( $R^2$ ) are better than 0.990) at all emission wavelengths above. The standard deviation in the identified  $T_g$  was typically less than 1.0 K.

The temperature of the film was adjusted with a temperature controller and a flat ribbon heater (Minco Products) mounted on a thin aluminium plate. The glass slide containing the PS film was held on the aluminium plate by a quartz cover slide placed on top of the films and a light clamping device. It is important to note that the film was only supported on one side during the measurement and that the film did not adhere to the cover quartz, indicating the film was in intimate contact only with the substrate on which it was originally placed. Fluorescence measurements of single-layer films were taken by first annealing the film at a minimum of  $T_g + 20$  K for 10 min and taking an emission intensity measurement at 5 K decrements (measurements are taken on cooling from the rubbery state), allowing 5 min at each temperature setting for thermal equilibrium to be achieved. Multilayer films were annealed at 403 K for 10 min before taking a measurement at that temperature, and then taking an emission intensity measurement at 5 K decrements (measurements are taken on cooling from the rubbery state), allowing 5 min for equilibration at each temperature setting. Additional aspects of this technique are reported elsewhere<sup>31,32</sup>.

Received 3 June 2003; accepted 12 August 2003; published 21 September 2003.

#### References

1. Angell, C. A., Ngai, K. L., McKenna, G. B., McMillan, P. F. & Martin, S. W. Relaxation in glassforming liquids and amorphous solids. *J. Appl. Phys.* **88**, 3113–3157 (2000).
2. Debenedetti, P. G. & Stillinger, F. H. Supercooled liquids and the glass transition. *Nature* **410**, 259–267 (2001).
3. Sillescu, H. Heterogeneity at the glass transition: A review. *J. Non-Cryst. Solids* **243**, 81–108 (1999).
4. Jackson, C. L. & McKenna, G. B. The glass transition of organic liquids confined to small pores. *J. Non-Cryst. Solids* **131**, 221–224 (1991).
5. Reiter, G. Mobility of polymers in films thinner than their unperturbed size. *Europhys. Lett.* **23**, 579–584 (1993).
6. Keddie, J. L., Jones, R. A. L. & Cory, R. A. Size-dependent depression of the glass transition temperature in polymer films. *Europhys. Lett.* **27**, 59–64 (1994).
7. Forrest, J. A. & Dalnoki-Veress, K. The glass transition in thin polymer films. *Adv. Coll. Interf. Sci.* **94**, 167–196 (2001).
8. Adam, G. & Gibbs, J. H. On temperature dependence of cooperative relaxation properties in glass-forming liquids. *J. Chem. Phys.* **43**, 139–146 (1965).
9. Hempel, E., Hempel, H., Hensel, A., Schick, C. & Donth, E. Characteristic length of dynamic glass transition near  $T_g$  for a wide assortment of glass-forming substances. *J. Phys. Chem. B* **104**, 2460–2466 (2000).
10. Reinsberg, S. A., Qui, X. H., Wilhelm, M., Spiess, H. W. & Ediger, M. D. Length scale of dynamic heterogeneity in supercooled glycerol near  $T_g$ . *J. Chem. Phys.* **114**, 7299–7302 (2001).
11. Arndt, M., Stannarius, R., Groothues, H., Hempel, E. & Kremer, F. Length scale of cooperativity in the dynamic glass transition. *Phys. Rev. Lett.* **79**, 2077–2080 (1997).
12. Barut, G., Pissis, P., Petster, R. & Nimtz, G. Glass transition in liquids: Two versus three-dimensional confinement. *Phys. Rev. Lett.* **80**, 3543–3546 (1998).
13. Melnichenko, Y. B., Schuller, J., Richert, R., Ewen, B. & Long, C. K. Dynamics of hydrogen-bonded liquids confined to mesopores: A dielectric and neutron spectroscopy study. *J. Chem. Phys.* **103**, 2016–2024 (1995).
14. Schonhals, A., Goering, H. & Schick, C. Segmental and chain dynamics of polymers: From the bulk to the confined state. *J. Non-Cryst. Solids* **305**, 140–149 (2002).
15. Kawana, S. & Jones, R. A. L. Character of the glass transition in thin supported polymer films. *Phys. Rev. E* **63**, 021501 (2001).
16. van Zanten, J. H., Wallace, W. E. & Wu, W. L. Effect of strongly favorable substrate interactions on the thermal properties of ultrathin polymer films. *Phys. Rev. E* **53**, R2053–R2056 (1996).
17. Fukao, K. & Miyamoto, Y. Glass transitions and dynamics in thin polymer films: dielectric relaxation of thin films of polystyrene. *Phys. Rev. E* **61**, 1743–1754 (2000).
18. Forrest, J. A., Dalnoki-Veress, K., Stevens, J. R. & Dutcher, J. R. Effect of free surfaces on the glass transition temperature of thin polymer films. *Phys. Rev. Lett.* **77**, 2002–2005 (1996).
19. DeMaggio, G. B. *et al.* Interface and surface effects on the glass transition in thin polystyrene films. *Phys. Rev. Lett.* **78**, 1524–1527 (1997).
20. Long, D. & Lequeux, F. Heterogeneous dynamics at the glass transition in van der Waals liquids, in the bulk and in thin films. *Eur. Phys. J. E* **4**, 371–387 (2001).
21. de Gennes, P. G. Glass transitions in thin polymer films. *Eur. Phys. J. E* **2**, 201–203 (2000).
22. Dalnoki-Veress, K., Forrest, J. A., de Gennes, P. G. & Dutcher, J. R. Glass transition reductions in thin freely-standing polymer films: A scaling analysis of chain confinement effects. *J. Phys. IV* **10**, 221–226 (2000).
23. Forrest, J. A. & Mattsson, J. Reductions of the glass transition temperature in thin polymer films: probing the length scale of cooperative dynamics. *Phys. Rev. E* **61**, R53–R56 (2000).
24. McCoy, J. D. & Curro, J. G. Conjectures on the glass transition of polymers in confined geometries. *J. Chem. Phys.* **116**, 9154–9157 (2002).
25. Torres, J. A., Nealey, P. F. & de Pablo, J. J. Molecular simulation of ultrathin polymeric films near the glass transition. *Phys. Rev. Lett.* **85**, 3221–3224 (2000).
26. Jones, R. A. L. Commentary to “Glass transitions in thin polymer films”. *Eur. Phys. J. E* **2**, 205 (2000).
27. Hall, D. B., Underhill, P. & Torkelson, J. M. Spin coating of thin and ultrathin polymer films. *Polym. Eng. Sci.* **38**, 2039–2045 (1998).
28. Frank, C. W. *et al.* Structure in thin and ultrathin spin-cast polymer films. *Science* **273**, 912–915 (1996).
29. Hall, D. B., Hooker, J. C. & Torkelson, J. M. Ultrathin polymer films near the glass transition: Effect on the distribution of alpha-relaxation times as measured by second harmonic generation. *Macromolecules* **30**, 667–669 (1997).
30. Schwab, A. D., Agra, D. M. G., Kim, J. H., Kumar, S. & Dhinojwala, A. Surface dynamics in rubbed polymer thin films probed with optical birefringence measurements. *Macromolecules* **33**, 4903–4909 (2000).
31. Ellison, C. J., Hall, D. B., Kim, S. D. & Torkelson, J. M. Confinement and processing effects on glass transition temperature and physical aging in ultrathin polymer films: Novel fluorescence measurements. *Eur. Phys. J. E* **8**, 155–165 (2002).
32. Ellison, C. J. & Torkelson, J. M. Sensing the glass transition in thin and ultrathin polymer films via fluorescence probes and labels. *J. Polym. Sci. B* **24**, 2745–2758 (2002).
33. Bell, R. C., Wang, H., Iedema, M. J. & Cowin, J. P. Nanometre-resolved interfacial fluidity. *J. Am. Chem. Soc.* **125**, 5176–5185 (2003).
34. Deschenes, L. A. & Vanden Bout, D. A. Single-molecule studies of heterogeneous dynamics in polymer melts near the glass transition. *Science* **292**, 255–258 (2001).
35. Quirin, J. C., Bartko, A. C., Dickson, R. M. & Torkelson, J. M. Signature of nanoscale dynamic heterogeneity in polymers near the glass transition: Non-gaussian displacement distribution from single-molecule probe diffusion studies. *Polym. Preprints* **42**(2), 174–175 (2001).
36. Deppe, D. D., Dhinojwala, A. & Torkelson, J. M. Small molecule probe diffusion in thin polymer films near the glass transition: A novel approach using fluorescence nonradiative energy transfer. *Macromolecules* **29**, 3898–3908 (1996).
37. Hall, D. B., Dhinojwala, A. & Torkelson, J. M. Translation-rotation paradox for diffusion in glass-forming polymers: The role of the temperature dependence of the relaxation times distribution. *Phys. Rev. Lett.* **79**, 103–106 (1997).
38. Whitlow, S. J. & Wool, R. P. Diffusion of polymers at interfaces – a secondary ion mass-spectroscopy study. *Macromolecules* **24**, 5926–5938 (1991).
39. Frank, B., Gast, A. P., Russell, T. P., Brown, H. R. & Hawker, C. Polymer mobility in thin films. *Macromolecules* **29**, 6531–6534 (1996).
40. X. Zheng *et al.* Long-range effects on polymer diffusion induced by a bounding interface. *Phys. Rev. Lett.* **79**, 241–244 (1997).
41. Jean, Y. C. *et al.* Glass transition of polystyrene near the surface studied by slow-positron-annihilation spectroscopy. *Phys. Rev. B* **56**, R8459–R8462 (1997).
42. Agra, D. M. G., Schwab, A. D., Kim, J. H., Kumar, S. & Dhinojwala, A. Relaxation dynamics of rubbed polystyrene thin films. *Europhys. Lett.* **51**, 655–660 (2000).
43. Wallace, W. E., Fischer, D. A., Efimko, K., Wu, W. L. & Genzer, J. Polymer chain relaxation: Surface outpaces bulk. *Macromolecules* **34**, 5081–5082 (2001).
44. Liu, Y. *et al.* Surface relaxations in polymers. *Macromolecules* **30**, 7768–7771 (1997).
45. Glotzer, S. C. Spatially heterogeneous dynamics in liquids: insights from simulation. *J. Non-Cryst. Solids* **274**, 342–355 (2000).
46. Weeks, E. R., Crocker, J. C., Levitt, A. C., Schofield, A. & Weitz, D. A. Three-dimensional imaging of structural relaxation near the colloidal glass transition. *Science* **287**, 627–631 (2000).
47. Yu, C. J., Richter, A. G., Datta, A., Durbin, M. K. & Dutta, P. Observation of molecular layering in thin liquid films using x-ray reflectivity. *Phys. Rev. Lett.* **82**, 2336–2339 (1999).
48. Russel, E. V. & Israeloff, N. E. Direct observation of molecular cooperativity near the glass transition. *Nature* **408**, 695–698 (2000).

Correspondence and requests for materials should be addressed to J.M.T.

#### Competing financial interests

The authors declare that they have no competing financial interests.